

# Self-assembly of DNA Nanohydrogels with Controllable Size and Stimuli-Responsive Property for Targeted Gene Regulation Therapy

Juan Li,<sup>†,‡</sup> Cheng Zheng,<sup>†</sup> Sena Cansiz,<sup>‡</sup> Cuichen Wu,<sup>‡</sup> Jiehua Xu,<sup>‡,⊥</sup> Cheng Cui,<sup>‡</sup> Yuan Liu,<sup>‡</sup> Weijia Hou,<sup>‡</sup> Yanyue Wang,<sup>‡</sup> Liqin Zhang,<sup>‡</sup> I-ting Teng,<sup>‡</sup> Huang-Hao Yang,<sup>\*,†</sup> and Weihong Tan<sup>\*,‡,§</sup>

<sup>†</sup>The Key Lab of Analysis and Detection Technology for Food Safety of the MOE, Fujian Provincial Key Laboratory of Analysis and Detection Technology for Food Safety, College of Chemistry, Fuzhou University, Fuzhou 350002, P.R. China

<sup>§</sup>Molecular Science and Biomedicine Laboratory, State Key Laboratory for Chemo/Bio-Sensing and Chemometrics, College of Chemistry and Chemical Engineering, College of Biology, and Collaborative Research Center of Molecular Engineering for Theranostics, Hunan University, Changsha 410082, P.R. China

<sup>‡</sup>Department of Chemistry and Physiology and Functional Genomics, Center for Research at the Bio/Nano Interface, Shands Cancer Center, University of Florida, Gainesville, Florida 32611-7200, United States

<sup>⊥</sup>Department of Nuclear Medicine, The Third Affiliated Hospital, Sun Yat-Sen University, Guangzhou 510630, P.R. China

## S Supporting Information

**ABSTRACT:** Here, we report the synthesis and characterization of size-controllable and stimuli-responsive DNA nanohydrogels as effective targeted gene delivery vectors. DNA nanohydrogels were created through a self-assembly process using three kinds of building units, respectively termed Y-shaped monomer A with three sticky ends (YMA), Y-shaped monomer B with one sticky end (YMB), and DNA linker (LK) with two sticky ends. Hybridization at the sticky ends of monomers and LK leads to nanohydrogel formation. DNA nanohydrogels are size-controllable by varying the ratio of YMA to YMB. By incorporating different functional elements, such as aptamers, disulfide linkages, and therapeutic genes into different building units, the synthesized aptamer-based nanohydrogels (Y-gel-Apt) can be used for targeted and stimuli-responsive gene therapy. Y-gel-Apt strongly inhibited cell proliferation and migration in target A549 cells, but not in control cells. By taking advantage of facile modular design and assembly, efficient cellular uptake, and superior biocompatibility, this Y-gel-Apt holds great promise as a candidate for targeted gene or drug delivery and cancer therapy.

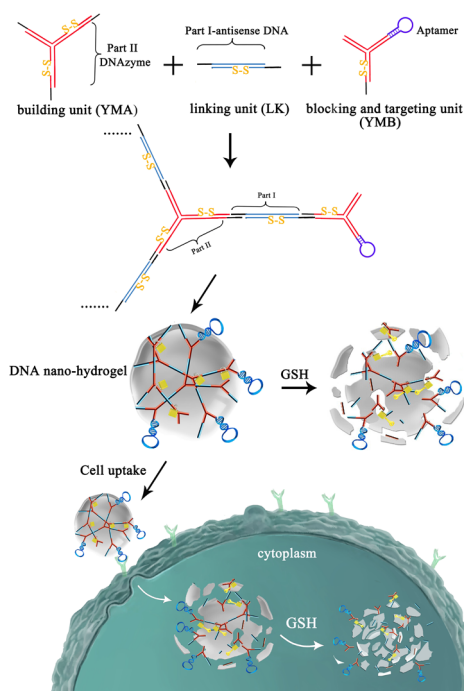
Gene regulation therapy is a promising approach for the treatment of both inherited and acquired diseases, such as cancers, hemophilia, and viral infections.<sup>1</sup> However, its success is largely dependent on the development of useful gene delivery vectors. Safety and efficiency of gene delivery vectors remain key technical barriers to the full exploitation of the potential of gene therapy.<sup>2</sup> Currently, gene therapy vectors mainly include two categories, viral vectors and nonviral vectors.<sup>3</sup> Viral vectors are widely used for efficient gene transfer; however, they are generally regarded as high risk based on safety issues, particularly immunogenicity and mutagenic toxicity. In some clinical situations, their use has resulted in patient death.<sup>4</sup> This has led to a surge in the development of nonviral vectors, which have been increasingly proposed as more desirable and safer

alternatives to viral vectors.<sup>5</sup> Nevertheless, compared with viral vectors, nonviral vectors exhibit significantly lower transfection efficiency, which greatly limits their clinical applications.<sup>6</sup> Therefore, the development of safe nonviral vectors capable of efficient transport and elevated therapeutics is highly desirable. Over the past decade, a variety of nonviral vectors, including liposomes,<sup>7</sup> dendrimers,<sup>8</sup> micelles,<sup>9</sup> inorganic nanoparticles,<sup>10</sup> DNA nanostructures,<sup>11</sup> and polymeric nanoparticles (named nanohydrogels),<sup>12</sup> have been investigated for their gene delivery potential. Among these, nanohydrogels have been explored as strong delivery vector candidates because of their high payload capacity, as well as biocompatibility, flexibility, and mechanical stability.<sup>13,14</sup> DNA- or RNA-functionalized hydrogels significantly expand the application fields of hydrogels and have attracted considerable attention in a wide range of biotechnological and biomedical uses, including biosensors,<sup>15–17</sup> controlled drug delivery,<sup>18</sup> RNA interference,<sup>19</sup> and tissue engineering.<sup>20</sup> However, the laborious and complicated modification steps for DNA-polymer hybrids have limited this progress. Previous research has shown that DNA hydrogels without synthetic polymers can also be created through enzyme ligation,<sup>21</sup> enzyme polymerization,<sup>22</sup> intermolecular i-motif structures,<sup>23</sup> and DNA hybridization.<sup>24</sup> These DNA hydrogels have been demonstrated for potential applications in drug release,<sup>21</sup> cell-free protein production,<sup>25</sup> and DNA immunotherapy.<sup>26</sup> However, the bulky size of DNA hydrogels and lack of efficient release mechanisms largely curtail their biomedical applications. In the present research, we developed a general approach to create DNA nanohydrogels with controllable size through self-assembly without any additional assistance. Based on this approach, we designed stimuli-responsive DNA nanohydrogels for targeted gene therapy.

As illustrated in Scheme 1, we designed three kinds of building units: Y-shaped monomer A (YMA), Y-shaped monomer B (YMB), and a DNA linker (LK). The YMA serves as a building unit, assembled from three single-stranded DNAs (ssDNAs),

Received: December 5, 2014

Published: January 12, 2015

Scheme 1. Schematic illustration of Stimuli-Responsive DNA Nanohydrogel Formation<sup>a</sup>

<sup>a</sup>The Y-shaped monomers (YMA and YMB) and linker are designed to crosslink by hybridization of their “sticky end” segments (black lines), leading to nanohydrogel formation.

and each strand has a “sticky end” segment (black lines) to hybridize with its complementary segment on LK (black lines). The YMB is also assembled from three ssDNAs. However, it has only one strand with a “sticky end” segment (black lines), while another strand consists of an aptamer. Aptamers are oligonucleic acid molecules generated from a process known as cell-based systematic evolution of ligands by exponential enrichment (SELEX) for specific recognition of certain cancer cells. Therefore, the YMB serves as both a blocking unit for inhibiting the extension of nanoparticles and a targeting unit for recognizing specific cancer cells. The LK is a linear duplex formed by two ssDNAs and contains two “sticky ends”. The “sticky ends” of the Y-shaped monomers and DNA linker are complementary to each other, and we propose that this hybridization leads to nanohydrogel formation. To design stimuli-responsive DNA nanohydrogels for targeted gene therapy, different functional elements, including antisense oligonucleotides capable of inhibiting cell proliferation,<sup>27</sup> DNAzymes capable of inhibiting cell migration,<sup>28</sup> and aptamers capable of targeting specific cancer cells,<sup>29</sup> can be incorporated into different building units. To achieve stimuli responsiveness in the DNA nanohydrogels, we incorporated disulfide linkages into Y-shaped monomers and LK, which are relatively stable during blood circulation and can be cleaved by the reducing agent GSH in the cytosol, thereby facilitating the selective release of therapeutic genes inside cells.<sup>30</sup> As a result, hundreds of therapeutic genes could be self-assembled into multifunctional nanohydrogels with controllable diameters, targeted delivery, and controllable release inside the target cells.

Based on previous reports,<sup>24</sup> we chose 13-base sticky ends to obtain a sufficiently stable assembled structure. To demonstrate the precise self-assembly of this modular approach, agarose gel

electrophoresis was used to examine the formation of each single building unit. The smaller mobility of monomers and LK was observed relative to ssDNA and partially assembled ssDNA (Figure S1; see Table S1 for detailed sequences). The results demonstrated that DNA monomers and LK were indeed formed as designed and that the assembly process was efficient by the presence of clean single bands (Figure 1a, lanes 1–3). When

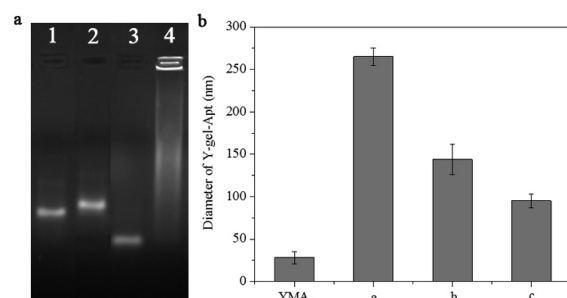


**Figure 1.** (a) Analysis by 3% agarose gel electrophoresis. Lane 1 is YMA, lane 2 is YMB, lane 3 is LK, and lane 4 is Y-gel-Apt with molar ratio of 4:1 (YMA/YMB). (b) Size-dependent (in diameter) distribution of hydrogel nanoparticles with different molar ratios of YMA and YMB: (a) 4:1 (NP-1), (b) 3:1 (NP-2), (c) 2:1 (NP-3).

YMA and YMB were mixed with LK, we observed an intense band in the sample loading zone, suggesting that a new high molecular weight DNA product was generated (Figure 1a, lane 4). This result revealed that self-assembly of Y-shaped monomers and LK can create larger DNA nanohydrogels composed of many copies of building units.

For further characterization of nanohydrogels, we used dynamic light scattering (DLS) and atomic force microscopy (AFM) to determine the average particle size and morphology. DLS revealed that the initial hydrodynamic diameter of YMA was 28 nm, but it increased to 265 nm after assembly with LK and YMB (Figure 1b). We further investigated the influence of the ratio of YMA to YMB on the size of the resulting DNA hydrogel nanoparticles. To accomplish this, YMA and YMB were mixed at different molar ratios, namely 4:1, 3:1, and 2:1. As shown in Figure 1b, the size of these nanoparticles could be controlled by varying the ratio of YMA to YMB. A higher ratio of YMB induces smaller nanoparticle diameters because YMB serves to block the extension of nanoparticles. Therefore, the different ratio of YMA to YMB leads to the formation of hydrogel nanoparticles having different sizes. These results correlated well with the average size obtained by AFM results (Figure S2), and all the nanohydrogels were found to have well-defined 3D spherical structures (Figure 2). Taking advantage of this strategy, DNA nanohydrogels can be prepared without enzymatic ligation or photopolymerization, thus reducing preparation time and damage to DNA. Therefore, the self-assembly approach is simple and useful for preparation of different DNA structures. The controllable size of the nanohydrogels is very important to their fate in the bloodstream. The sub-200 nm size is desirable for nanoparticles to extend their blood circulation time.<sup>31</sup> Accordingly, 144 nm nanohydrogels (NP-2) were used for subsequent experiments.

To examine whether DNA nanohydrogels were degradable in the intracellular reductive environment, where the concentration of GSH is maintained at a relatively high concentration (0.5 to 10 mM),<sup>32</sup> DNA nanohydrogels exposed to GSH were characterized by agarose gel. DNA nanohydrogels were primarily located in the loading zone, but after treatment with GSH to

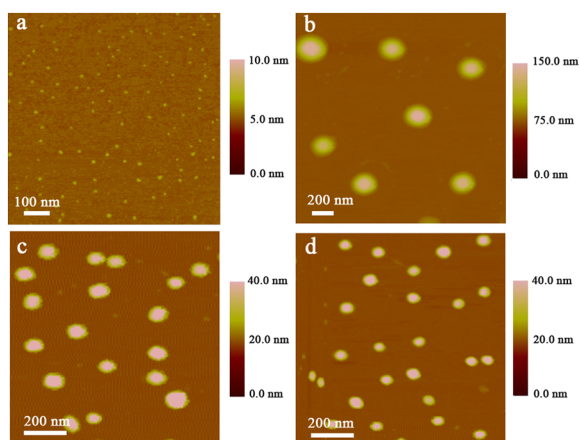


**Figure 2.** AFM images of YMA (a) and DNA hydrogel nanoparticles with different molar ratios of YMA to YMB: (b) 4:1 (NP-1), (c) 3:1 (NP-2), (d) 2:1 (NP-3).

cleave disulfide linkages, DNA fractions appeared in the agarose gel (Figure S3). Similar results were observed for Y-shaped monomer and DNA linker (Figure S3). These results demonstrated that the disulfide linkages incorporated in the monomers, LK, and nanohydrogels were efficiently cleaved in the intracellular reductive environment, resulting in dissociation of DNA nanohydrogels and release of multiple therapeutic genes.

To verify the feasibility of DNA nanohydrogels as targeted gene delivery vectors, a cancer cell-specific DNA aptamer was selected as the targeting recognition molecule. As a proof of concept, S6 aptamer,<sup>29</sup> which targets A549 cancer cells (human lung adenocarcinoma epithelial cell line), but not HeLa cells, was conjugated into the YMB. FITC-labeled S6 was synthesized to provide a means of fluorescent tracing. The selective binding affinity of DNA nanohydrogels with aptamers (named Y-gel-Apt) was verified by flow cytometry. Figure 3a shows a large fluorescence signal shift for A549 cells treated with Y-gel-Apt, while no significant shift was observed for HeLa cells (Figure 3b). The results of confocal laser scanning microscopy (CLSM) were

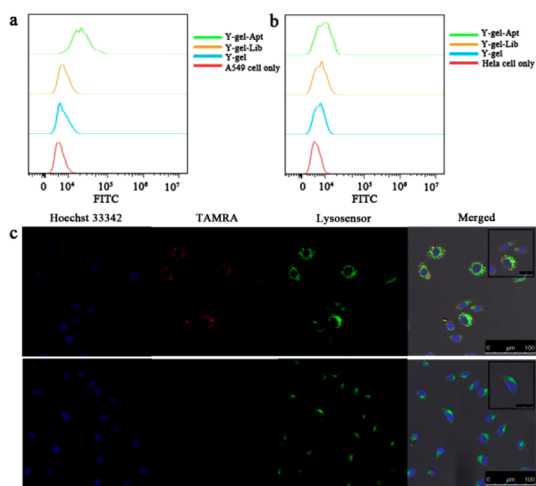


**Figure 3.** Flow cytometry histograms to monitor the binding of Y-gel-Apt with (a) A549 cells and (b) HeLa cells. (c) Confocal laser scanning microscopy images of the colocalization of TAMRA-labeled Y-gel-Apt and lysosensor (lysosome marker), indicating the specific internalization of Y-gel-Apt into A549 cells (top) rather than HeLa cells (bottom). Scale bar represents 100  $\mu\text{m}$ , and inset bar represents 25  $\mu\text{m}$ .

consistent with those of flow cytometry (Figure 3c). After incubating A549 cells with Y-gel-Apt for 2 h, a strong red fluorescence was observed by CLSM, but no distinct red fluorescence was observed for HeLa cells (Figure 3c). Thus, the aptamer-based nanohydrogel has properties of a large nanostructure, including selective targeting and internalization, making it a potential platform for targeted gene delivery.

We further investigated the utility of this vector for targeted gene regulation therapy. As a proof of concept, we incorporated two different kinds of therapeutic genes into YMA and LK, respectively. The first was a therapeutic antisense oligonucleotide against c-raf-1 mRNA, which is a cancer biomarker and antisense therapeutic target of great significance in cancer diagnostics and therapeutics.<sup>27</sup> The antisense oligonucleotides were conjugated into LK. The other was a DNzyme targeting matrix metalloproteinase-9 (MMP-9), which is significantly associated with human nonsmall cell lung cancer (NSCLC) proliferation, invasion and metastasis.<sup>28</sup> DNzyme oligonucleotides were conjugated into YMA. Then, we evaluated the effect of Y-gel-Apt on cell proliferation and migration in A549 cells. According to the cytotoxicity assay (Figure 4), A549 cell growth was only

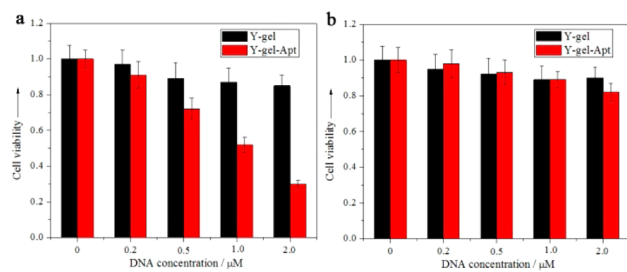


**Figure 4.** Cytotoxicity assay of (a) A549 cells and (b) HeLa cells treated with Y-gel-Apt and Y-gel at different concentrations.

negligibly influenced by the treatment of cells with Y-gel (without aptamers), indicating the excellent biocompatibility of these DNA nanohydrogels. However, treatment with Y-gel-Apt resulted in a marked inhibition of cell proliferation in a dose-dependent manner, suggesting that Y-gel-Apt could be selectively internalized into cells and that the antisense and DNzyme oligonucleotides transported by Y-gel-Apt played an important role in inhibiting cell proliferation.

The DNzyme oligonucleotides incorporated into Y-gel-Apt silenced the expression of complementary target mRNA by inducing mRNA cleavage and a subsequent decrease in target protein expression levels. As shown in Figure 5a, the expression of MMP-9 protein was strongly decreased in A549 cells by transfection with Y-gel-Apt compared with Y-gel and control. In contrast, Y-gel-Apt had negligible effect on the expression of MMP-9 protein in HeLa cells. These results demonstrated that Y-gel-Apt was capable of modulating protein expression in a target-specific manner.

To provide further support for the effect of Y-gel-Apt targeting of MMP-9 protein by DNzyme, we used an *in vitro* scratch wound healing assay, in which the extent of cell migration into the scratched area was measured. The results are shown in Figure 5b. The migration of A549 cells was effectively inhibited by treatment with Y-gel-Apt compared to cells treated with Y-gel and control. However, a slight inhibition of migration was also observed, possibly because of the nonspecific internalization of Y-gel during a long incubation period. These results revealed that the Y-gel-Apt treatment remarkably inhibited cell proliferation



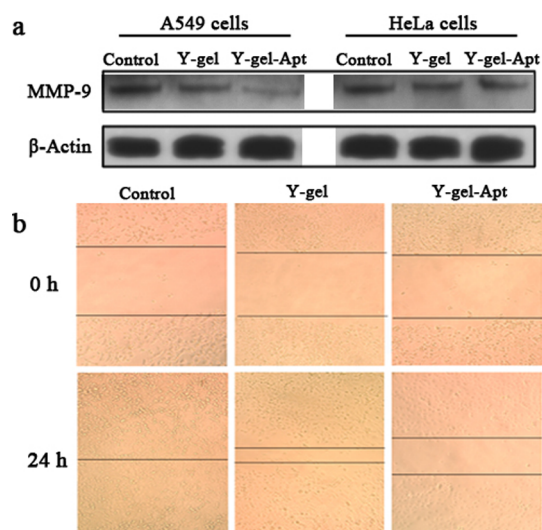


**Figure 5.** (a) Western blot analysis of MMP-9 protein expression in A549 cells and HeLa cells with Y-gel-Apt and Y-gel treatments.  $\beta$ -Actin serves as a control for equal protein loading. (b) *In vitro* scratch wound healing assay. Y-gel-Apt inhibits the migration of A549 cells *in vitro*.

and migration of the A549 cells, suggesting that Y-gel-Apt can be considered as a potential candidate for targeted gene therapy.

In summary, this study has demonstrated that two kinds of Y-shaped monomers and DNA linker can self-assemble in a one-step reaction to generate DNA nanohydrogels with controllable size. By incorporating different functional elements, such as aptamers, disulfide linkages, and therapeutic genes into different building units, the synthesized Y-gel-Apt can be used for targeted and stimuli-responsive gene regulation therapy, resulting in the inhibition of cell proliferation and migration in A549 cells. The advantages of these DNA nanohydrogels include easy synthesis without enzymatic ligation or photopolymerization, controlled size, efficient cellular uptake, enhanced nuclease resistance (Figure S4), and superior biocompatibility. Furthermore, these nanohydrogels can be used as safe nanocarriers for the delivery of drug or imaging agents. Thus, the proposed multifunctional aptamer-based DNA nanohydrogels will find potential applications for point-of-care diagnosis, efficient drug transport, and improved targeted cancer therapeutics.

## ■ ASSOCIATED CONTENT

### 📄 Supporting Information

Experimental details and additional characterization data. This material is available free of charge via the Internet at <http://pubs.acs.org>.

## ■ AUTHOR INFORMATION

### Corresponding Authors

\*tan@chem.ufl.edu

\*hhyang@fzu.edu.cn

### Notes

The authors declare no competing financial interest.

## ■ ACKNOWLEDGMENTS

This work is supported by grants awarded by the National Institutes of Health (GM079359 and CA133086), by the National Key Scientific Program of China (2011CB911000 and No. 2010CB732403), NSFC grants (NSFC 21221003, NSFC 21327009 and NSFC 21125524) and China National

Instrumentation Program 2011YQ03012412. C.W. acknowledges the support from the American Chemical Society, Division of Analytical Chemistry Fellowship, sponsored by the Society for Analytical Chemists of Pittsburgh.

## ■ REFERENCES

- (1) Verma, I. M.; Somia, N. *Nature* **1997**, *389*, 239.
- (2) Li, S.; Huang, L. *Gene Ther.* **2000**, *7*, 31.
- (3) Cavazzana-Calvo, M.; Thrasher, A.; Mavilio, F. *Nature* **2004**, *427*, 779.
- (4) Waehler, R.; Russell, S. J.; Curiel, D. T. *Nat. Rev. Genet.* **2007**, *8*, 573.
- (5) Mintzer, M. A.; Simanek, E. E. *Chem. Rev.* **2009**, *109*, 259.
- (6) Alexander, B. L.; Ali, R. R.; Alton, E. W.; Bainbridge, J. W.; Braun, S.; Cheng, S. H.; Flotte, T. R.; Gaspar, H. B.; Grez, M.; Griesenbach, U.; Kaplitt, M. G.; Ott, M. G.; Seger, R.; Simons, M.; Thrasher, A. J.; Thrasher, A. Z.; Yla-Herttuala, S. *Gene Ther.* **2007**, *14*, 1439.
- (7) Torchilin, V. P. *Nat. Rev. Drug Discovery* **2005**, *4*, 145.
- (8) Joester, D.; Losson, M.; Pugin, R.; Heinzelmann, H.; Walter, E.; Merkle, H. P.; Diederich, F. *Angew. Chem., Int. Ed.* **2003**, *42*, 1486.
- (9) Chen, T.; Wu, C. S.; Jimenez, E.; Zhu, Z.; Dajac, J. G.; You, M.; Han, D.; Zhang, X.; Tan, W. *Angew. Chem., Int. Ed.* **2013**, *52*, 2012.
- (10) Sokolova, V.; Epple, M. *Angew. Chem., Int. Ed.* **2008**, *47*, 1382.
- (11) Wu, C.; Han, D.; Chen, T.; Peng, L.; Zhu, G.; You, M.; Qiu, L.; Sefah, K.; Zhang, X.; Tan, W. *J. Am. Chem. Soc.* **2013**, *135*, 18644.
- (12) Dunn, S. S.; Tian, S.; Blake, S.; Wang, J.; Galloway, A. L.; Murphy, A.; Pohlhaus, P. D.; Rolland, J. P.; Napier, M. E.; DeSimone, J. M. *J. Am. Chem. Soc.* **2012**, *134*, 7423.
- (13) Nuhn, L.; Hirsch, M.; Krieg, B.; Koynov, K.; Fischer, K.; Schmidt, M.; Helm, M.; Zentel, R. *ACS Nano* **2012**, *6*, 2198.
- (14) Dahlman, J. E.; et al. *Nat. Nanotechnol.* **2014**, *9*, 648.
- (15) Yang, H.; Liu, H.; Kang, H.; Tan, W. *J. Am. Chem. Soc.* **2008**, *130*, 6320.
- (16) Zhu, Z.; Wu, C.; Liu, H.; Zou, Y.; Zhang, X.; Kang, H.; Yang, C. J.; Tan, W. *Angew. Chem., Int. Ed.* **2010**, *49*, 1052.
- (17) Yan, L.; Zhu, Z.; Zou, Y.; Huang, Y.; Liu, D.; Jia, S.; Xu, D.; Wu, M.; Zhou, Y.; Zhou, S.; Yang, C. J. *J. Am. Chem. Soc.* **2013**, *135*, 3748.
- (18) Kang, H.; Trondoli, A. C.; Zhu, G.; Chen, Y.; Chang, Y. J.; Liu, H.; Huang, Y. F.; Zhang, X.; Tan, W. *ACS Nano* **2011**, *5*, 5094.
- (19) Lee, J. B.; Hong, J.; Bonner, D. K.; Poon, Z.; Hammond, P. T. *Nat. Mater.* **2012**, *11*, 316.
- (20) Shea, L. D.; Smiley, E.; Bonadio, J.; Mooney, D. J. *Nat. Biotechnol.* **1999**, *17*, 551.
- (21) Um, S. H.; Lee, J. B.; Park, N.; Kwon, S. Y.; Umbach, C. C.; Luo, D. *Nat. Mater.* **2006**, *5*, 797.
- (22) Lee, J. B.; Peng, S.; Yang, D.; Roh, Y. H.; Funabashi, H.; Park, N.; Rice, E. J.; Chen, L.; Long, R.; Wu, M.; Luo, D. *Nat. Nanotechnol.* **2012**, *7*, 816.
- (23) Cheng, E.; Xing, Y.; Chen, P.; Yang, Y.; Sun, Y.; Zhou, D.; Xu, L.; Fan, Q.; Liu, D. *Angew. Chem., Int. Ed.* **2009**, *48*, 7660.
- (24) Xing, Y.; Cheng, E.; Yang, Y.; Chen, P.; Zhang, T.; Sun, Y.; Yang, Z.; Liu, D. *Adv. Mater.* **2011**, *23*, 1117.
- (25) Park, N.; Um, S. H.; Funabashi, H.; Xu, J.; Luo, D. *Nat. Mater.* **2009**, *8*, 432.
- (26) Nishikawa, M.; Mizuno, Y.; Mohri, K.; Matsuoka, N.; Rattanakit, S.; Takahashi, Y.; Funabashi, H.; Luo, D.; Takakura, Y. *Biomaterials* **2011**, *32*, 488.
- (27) Monia, B. P.; Johnston, J. F.; Geiger, T.; Muller, M.; Fabbro, D. *Nat. Med.* **1996**, *2*, 668.
- (28) Yang, L.; Zeng, W.; Li, D.; Zhou, R. *Oncol. Rep.* **2009**, *22*, 121.
- (29) Shi, H.; Cui, W.; He, X.; Guo, Q.; Wang, K.; Ye, X.; Tang, J. *PLoS One* **2013**, *8*, e70476.
- (30) Lee, M. H.; Yang, Z.; Lim, C. W.; Lee, Y. H.; Dongbang, S.; Kang, C.; Kim, J. S. *Chem. Rev.* **2013**, *113*, 5071.
- (31) Pouton, C. W.; Seymour, L. W. *Adv. Drug Delivery Rev.* **2001**, *46*, 187.
- (32) Wu, G.; Fang, Y. Z.; Yang, S.; Lupton, J. R.; Turner, N. D. *J. Nutr.* **2004**, *134*, 489.